A Head-to-Head Comparison of ^{68}Ga-DOTA-FAPI-04 and ^{18}F-FDG PET/MR in Patients with Nasopharyngeal Carcinoma: A Prospective Study

Chunxia Qin
Wuhan Union Hospital
Fang Liu
Wuhan Union Hospital
Jing Huang
Wuhan Union Hospital Oncology Center
Weiwei Ruan
Wuhan Union Hospital
Qingyao Liu
Wuhan Union Hospital
Yongkang Gai
Wuhan Union hospital
Fan Hu
Wuhan Union hospital
Dawei Jiang
Wuhan Union hospital
Yu Hu
Wuhan union hospital
Kunyu Yang
Wuhan Union Hospital Oncology Center
Xiaoli Lan (xiaoli_lan@hust.edu.cn)
Union Hospital, Tongji Medical College, Huazhong University of Science & Technology https://orcid.org/0000-0002-7263-7399

Research Article

Keywords: 68Ga-DOTA-FAPI-04, 18F-FDG, PET/MR, nasopharyngeal carcinoma, staging

Posted Date: March 2nd, 2021

DOI: https://doi.org/10.21203/rs.3.rs-252484/v1

Version of Record: A version of this preprint was published at European Journal of Nuclear Medicine and Molecular Imaging on February 20th, 2021. See the published version at https://doi.org/10.1007/s00259-021-05255-w.

Abstract

Purpose

To conduct a head-to-head comparison of the diagnostic ability of ^{68}Ga-DOTA-FAPI-04 (^{68}Ga-FAPI) and ^{18}F-FDG PET/MR in nasopharyngeal carcinoma (NPC) patients.

Methods

Patients diagnosed with NPC were prospectively enrolled. All patients underwent head-and-neck ^{68}Ga-FAPI PET/MR and ^{18}F-FDG PET/MR within one week. Primary tumor, lymph node numbers, and tracer uptake were compared by SUVmax and visual evaluation. The primary tumor volumes derived from ^{68}Ga-FAPI, ^{18}F-FDG PET, and MRI were also compared.

Results

Fifteen patients were enrolled from June to August 2020. Both ^{68}Ga-FAPI and ^{18}F-FDG PET had 100% detection rate of the primary tumor. The ^{68}Ga-FAPI SUVmax of primary tumors (13.87±5.13) was lower than that of ^{18}F-FDG (17.73±6.84), but the difference was not significant (p=0.078). Compared with ^{18}F-FDG, ^{68}Ga-FAPI PET improved the delineation of skull-base invasion in eight out of eight patients and intracranial invasion in four out of four patients. When 25%SUVmax of ^{68}Ga-FAPI or 20%SUVmax of ^{18}F-FDG was utilized as a threshold for determining tumor volume, it was highly consistent with MRI. ^{18}F-FDG PET detected much more positive lymph nodes than ^{68}Ga-FAPI (100 vs 48). The SUVmax of 48 paired lymph nodes was significantly lower on ^{68}Ga-FAPI than ^{18}F-FDG (8.67±3.88 vs 11.79±6.17, p<0.001). Additionally, ^{68}Ga-FAPI further detected four highly suspected small, distant metastases in three patients. Compared with ^{18}F-FDG, ^{68}Ga-FAPI changed overall staging in six of fifteen patients, with three patients being up-staged, and three down-staged.

Conclusion

^{68}Ga-FAPI outperforms ^{18}F-FDG in delineating the primary tumor and detecting suspected distant metastases, particularly in the evaluation of skull-base and intracranial invasion, suggesting ^{68}Ga-FAPI hybrid PET/MR has the potential to serve as a single-step staging modality for patients with NPC. However, its value regarding lymph node and distant metastases evaluation needs further study.

Trial registration: NCT04554719. Registered September 8, 2020 - retrospectively registered, http://clinicaltrails.gov/show/ NCT04554719

Introduction

Nasopharyngeal carcinoma (NPC) is a common malignancy in East and Southeast Asia, and particularly in southern China [1]. In patients with localized, advanced-stage disease, it is characterized by a high rate of skull-base and intracranial invasion. Determining the extent of tumor invasion and staging by noninvasive imaging techniques are critical for treatment choice and subsequent planning [2, 3].

Both magnetic resonance imaging (MRI) and fluorine-18 fludeoxyglucose (^{18}F-FDG) PET/CT are established imaging modalities for NPC management which are currently recommended for use in NPC staging by the National Comprehensive Cancer Network (NCCN) [3]. ^{18}F-FDG is the most frequently utilized tracer in PET imaging [4]. However, due to high physiologic glucose uptake in the brain and some healthy tissues [5], and the fact that CT has limited soft-tissue resolution compared with MRI, the sensitivity of ^{18}F-FDG PET/CT for the T staging of NPC is inadequate, particularly when characterizing skull-base and intracranial invasion [6]. Hybrid PET/MR is a new modality that acquires MR and PET images simultaneously, providing high soft-tissue contrast and multi-parametric information regarding the disease. Several studies have investigated the feasibility and clinical potential of ^{18}F-FDG PET/MR in NPC and have found it superior to PET/CT and head-and-neck MRI for assessing the extension of the primary tumor into the parapharyngeal spaces, skull-base, intracranial area, and nodal metastases. Therefore, PET/MR could serve as a reliable, one-step imaging examination for NPC assessment [7-9].

Gallium-68 labeled fibroblast-activation-protein inhibitor (^{68}Ga-FAPI) has recently been introduced as a promising tumor imaging agent targeting cancer-associated fibroblasts [10, 11]. A high uptake of radioactive FAPI has been confirmed in many types of tumors, including head-and-neck cancers [10, 12, 13]. However, there are currently no studies that evaluate the use of ^{68}Ga-FAPI PET for NPC. Additionally, the background level of ^{68}Ga-FAPI in the normal brain is reported to be very low [12]. We hypothesize, therefore, that ^{68}Ga-FAPI has good diagnostic value in NPC. In this study, we conducted a prospective study to investigate whether simultaneous ^{68}Ga-FAPI head-neck PET/MR is better than ^{18}F-FDG PET/MR for detecting primary tumor invasion, lymph node involvement, and distant metastases in NPC patients, and to explore the clinical impact (TNM staging) of ^{68}Ga-FAPI PET/MR compared with ^{18}F-FDG PET/MR.

Materials And Methods

Patients

This prospective study was approved by our hospital's Institutional Review Board (IRB 20200290). All patients signed an informed consent form prior to participation in the study. The inclusion criteria were patients (1) with histologically proven NPC, and (2) who had no anti-tumor therapy four weeks prior to

the examination. Exclusion criteria included patients (1) who had other primary malignancies at the time of examination, (2) with a history of neck surgery, (3) who suffered from hyperglycemia or severe hepatic and renal insufficiency, or (4) had contraindications for MRI.

^{18}F-FDG PET/MR and ^{68}Ga-FAPI PET/MR acquisition

All patients had fasted for at least 6 h before ^{18}F-FDG administration. Blood glucose was tested to ensure a normal blood glucose level. Whole-body (from top of head to mid-thigh) PET/CT was performed approximately 60 min after the intravenous injection of ^{18}F-FDG (3.7–5.4 MBq/kg, 0.10-0.15 mCi /kg) according to the clinical standard protocol for tumor imaging. Head-and-neck (from the suprasellar cistern to the sternoclavicular joint) ^{18}F-FDG PET/MR was subsequently performed on a hybrid time-of-flight (TOF) PET/MR scanner (SIGNA™ PET/MR, GE Healthcare, Waukesha, WI, USA). All patients underwent head-neck ^{68}Ga-FAPI PET/MR within one week, with no specific preparation required before ^{68}Ga-FAPI administration. The PET/MR scan was performed approximately 30–60 min after the intravenous injection of ^{68}Ga-FAPI (1.85-3.7 MBq/kg, 0.05-0.1 mCi /kg).

Both ^{18}F-FDG and ^{68}Ga-FAPI PET acquisitions were performed in 3D with a 10-min/bed position (DFOV=30 cm) during MR acquisition. The PET datasets were reconstructed with a 192×192 matrix (pixel size: 1.5625×1.5625×2.78 mm^3) with TOF and point spread function (PSF)-ordered subset expectation maximization (OSEM) algorithms with 28 subsets and three iterations, followed by a 3-mm Gaussian filter. A 32-channel head-neck united coil was used and the MRI sequences included axial and sagittal T1-weighted imaging (fast spin echo, TE/TR=14/500 ms, section thickness 4 mm), coronal T1-weighted imaging (fat-suppression fast spin echo, TE/TR=10/500 ms, section thickness 4 mm), axial T2-weighted imaging (fast spin echo, TE/TR=90/5000 ms, section thickness 4 mm), and coronal T2-weighted imaging (fat-suppression fast spin echo, TE/TR=90/5000 ms, section thickness 4 mm). The matrix of the axial plane was 320×224, and the matrix of the sagittal and coronal plane was 288×192. Contrast-enhanced MR was performed during either ^{18}F-FDG PET/MR or ^{68}Ga-FAPI PET/MR using an intravenous bolus injection of gadolinium-diethylenetriamine pentaacetic acid (gadolinium-EDTA, Gd-DTPA; 0.1 mmol/kg, 1.5ml/s, Magnevist, Bayer, USA). Axial and coronal T1-weighted images were acquired.

Imaging interpretation

The acquired PET and MR images were sent to the AW workstation (AW4.6, GE Healthcare, USA) for registration, fusion, and measurement. Both ^{18}F-FDG and ^{68}Ga-FAPI PET/MR images were visually evaluated by two experienced nuclear medicine physicians (C.Q. with 12 years of experience in nuclear oncology, and F.L. with 20 years of experience in MR and 5 years of experience in nuclear oncology) who are aware of clinical information of patients. The two reviewers conducted a frame-by-frame comparative analysis of the fused images of ^{18}F-FDG PET/MR and ^{68}Ga-FAPI PET/MR, and reached a final TNM diagnosis based mainly on the fusion images. Any initial differences of opinion were resolved by consensus.

(1) T staging assessment: According to the NCCN guidelines [3], contrast-enhanced MR images are the gold standard for evaluating primary lesions and their invasion of adjacent tissues. Compared with contrast-enhanced MR images, a lesion showing ^{18}F-FDG or ^{68}Ga-FAPI uptake that exceeded uptake in the adjacent tissue was considered to have tumor infiltration. The region of interest of the primary tumor was manually drawn along the margin of the lesion on the axial contrast-enhanced MR images and T2-weighted images because of their clear tumor borders. The maximum standardized uptake value (SUVmax) of the region of interest was measured on the PET images. The tumor volume shown on the PET images was calculated based on SUV thresholds of 20%, 25%, and 30% of SUVmax, respectively.

(2) N staging assessment: On MR images, the diagnosis of metastatic lymph nodes should satisfy at least one of the following criteria: (a) necrosis or extracapsular spread was observed, (b) the shortest axial diameter was ≥5 mm in the retropharyngeal region or ≥10 mm in other regions, (c) there was a cluster of three or more lymph nodes of borderline size [14]. On PET images, if ^{18}F-FDG or ^{68}Ga-FAPI uptake exceeded the surrounding tissue, it was regarded as a positive lymph node uptake. The site and number of positive lymph nodes were recorded and compared between the modalities.

(3) M staging assessment: The presence of distant metastases was determined based on the tracer uptake and MR signal intensity abnormalities. The site of the metastases was also recorded.

Statistics

All analyses were performed using the SPSS statistical package (version 22.0; SPSS, Chicago, IL, USA). Differences in SUVmax between groups were determined using a paired t-test. Two-tailed p-values of less than 0.05 were considered statistically significant.

Results

Patient cohort

Fifteen patients—eight men and seven women, aged from 36 to 69 years (mean 51.2 ± 9.4 years)—were included in this study from June to August 2020. The median time interval between the two scans was 1 day (range 1-3 days). All patients tolerated ^{68}Ga-FAPI and ^{18}F-FDG PET/MR well, and no ^{68}Ga-FAPI-related adverse effects were observed. **Table 1** shows the clinical information and the MR, ^{18}F-FDG, and ^{68}Ga-FAPI PET-based TNM staging of all the patients. Of the 15 patients, 14 were newly diagnosed with NPC, in which three cases were well-differentiated keratinizing squamous cell carcinoma (WHO Type I), two cases were nonkeratinizing differentiated carcinoma (WHO Type II), eight cases were nonkeratinizing undifferentiated carcinoma (WHO Type III), and one case was keratinizing carcinoma with unknown differentiation status. The other case was recurrent NPC with an unknown pathological type,

the patient was diagnosed in 2016 and underwent radiotherapy which ended in the same year. No distant metastases were revealed on whole-body ^{18}F-FDG PET/CT in any of the patients.

Primary tumor Detection and Visual Evaluation of Primary Tumor Invasion

^{18}F-FDG and ^{68}Ga-FAPI had equivalent detection ability for primary tumor in all NPC patients with 100% positive detection rate. **Figure 1** shows the images of four representative patients. Primary tumor uptake was higher in ^{18}F-FDG (SUVmax 17.73 ± 6.84) than ^{68}Ga-FAPI (SUVmax 13.87 ± 5.13), but no significant differences were found (P =0.078, **Table 2**). We further compared the correlation between the uptake of two tracers and found that the SUVmax of ^{68}Ga-FAPI had no relationship with ^{18}F-FDG (r =0.227, p=0.416, **Figure 2A**). The T staging of ^{68}Ga-FAPI was consistent with the MRI findings in all the patients, but the T staging in one of the patients was underestimated by ^{18}F-FDG (**Table 1**).

A visual evaluation of primary tumor invasion with two tracers was conducted (**Table 3**). All 15 patients had nasopharyngeal invasion with significant uptake on both ^{68}Ga-FAPI and ^{18}F-FDG. The invasion extent and the borders of the lesions were clearly delineated by both modalities, comparable to MR. However, when comparing the ^{68}Ga-FAPI and ^{18}F-FDG PET images, a visual evaluation was discordant in ten patients. ^{68}Ga-FAPI was found to be superior to ^{18}F-FDG in six of the 15 patients (40%) and inferior to ^{18}F-FDG in four patients (26.7%).

Twelve patients had a parapharyngeal space invasion. The tumor extent revealed by ^{68}Ga-FAPI PET in all patients was comparable to MR, whereas the ^{18}F-FDG images of two patients were inferior to the MR images. The number of cases of ^{68}Ga-FAPI that were superior, equivalent, and inferior to ^{18}F-FDG were five, two, and five, respectively. **Figure 3** shows an example of parapharyngeal space invasion, with a greater extent on ^{68}Ga-FAPI PET and MR than ^{18}F-FDG PET.

Eight patients had skull-base invasion. ^{68}Ga-FAPI PET showed comparable accuracy to that of head-and-neck MRI for detecting the involvement of the skull base in seven out of eight patients. In all eight patients (100%), both ^{68}Ga-FAPI PET and MR showed a larger extent or a clearer border of skull-base invasion than ^{18}F-FDG PET (**Figure 4**).

Four patients had intracranial invasion, which was clearly visualized by ^{68}Ga-FAPI PET and MR. However, ^{18}F-FDG PET was either negative or indeterminate because of the physiologic uptake of ^{18}F-FDG in the brain (**Figure 5**).

Comparison of primary tumor volume between the modalities

As shown in **Table 4** and **Table 5**, tumor volume measured by contrast-enhanced MRI and T2-weighted images were highly consistent (intraclass correlation coefficient, ICC 0.93), which indicates that the volumes measured by enhanced MR and T2-weighted images had a high level of credibility. The delineation volume of ^{68}Ga-FAPI 25%SUVmax and ^{18}F-FDG 20%SUVmax as thresholds had the highest credibility and consistency level with the volume measured by MR (Table 5, ICC 0.85-0.91).

Regional lymph node assessment

Of the 14 patients with suspected lymph node metastases, 78.6% (11/14) showed more positive lymph nodes on ^{18}F-FDG than on ^{68}Ga-FAPI, whereas 21.4% (3/14) demonstrated comparable results. Altogether, 100 and 48 positive lymph nodes were depicted by ^{18}F-FDG and ^{68}Ga-FAPI PET, respectively (p<0.001; **Table 2**). All ^{68}Ga-FAPI positive lymph nodes were ^{18}F-FDG positive. In all 48 double-positive lymph nodes, ^{18}F-FDG demonstrated significantly higher uptake than ^{68}Ga-FAPI (11.94±6.15 vs 8.81±3.79, p<0.001). A significant correlation was found between the two tracers concerning nodal uptake (**Figure 2B**, r= 0.512, p< 0.001). In all, compared with MR, ^{68}Ga-FAPI and ^{18}F-FDG PET led to upstaging of N stage in 20.0% (3/15) and 73.3% (11/15) patients, respectively. ^{18}F-FDG PET led to N upstaging in 53.3% (8/15) patients compared with ^{68}Ga-FAPI.

Distant metastases

^{68}Ga-FAPI was superior to ^{18}F-FDG in 100% (3/3) of the patients with suspected distant metastases. ^{68}Ga-FAPI aided the detection of three small skull lesions in two patients, which were initially overlooked during MRI interpretation and false-negative on the ^{18}F-FDG PET images (**Figure 6**). In another patient, a small suspicious metastasis on the pons was detected by ^{68}Ga-FAPI and enhanced MRI, which was missed by ^{18}F-FDG PET because of high physiologic uptake.

Changes in the overall staging

Overall, compared with ^{18}F-FDG, ^{68}Ga-FAPI led to the NPC being up-staged to Stage IVB in three patients because of the detection of small, distant suspicious metastases, and down-staging in three patients because of the relatively low positive rate of lymph nodes. Interestingly, when the highest stage from the three modalities was regarded as the final stage of the patient, we found ^{18}F-FDG SUVmax of the primary tumors of Stage IVB patients (26.73±5.17, n=3) was significantly higher than that of Stage II and III patients (15.58±3.53, n=5) and Stage IVA patients (15.40±6.41, n=7). In contrast, the differences of ^{68}Ga-FAPI SUVmax among groups were not significant (Stage I and II, 14.44±8.74; Stage IVA, 13.81±3.14; Stage IVB, 13.06±0.45).

Discussion

In this study, we prospectively compared the diagnostic and staging effectiveness of ^{68}Ga-FAPI and ^{18}F-FDG head-and-neck PET/MR in NPC patients. Our results showed that ^{68}Ga-FAPI was superior to ^{18}F-FDG in assessing skull-base and intracranial invasion and the small metastases on the skull and brain, which changed the overall staging in six patients. This suggested that ^{68}Ga-FAPI PET/MR may be another viable imaging candidate for diagnosing NPC. However, its value for N and M staging needs to be further explored.

The primary tumor in NPC can be visualized by both ^{18}F-FDG and ^{68}Ga-FAPI. Although ^{18}F-FDG showed higher uptake than ^{68}Ga-FAPI, the difference was not significant. Interestingly, no correlation was found in the primary tumor uptake values of the two tracers, which may be explained by different principles. ^{18}F-FDG reflects the glucose utilization of the lesion [4], but ^{68}Ga-FAPI reflects the activity of the cancer-associated fibroblast [11]. ^{68}Ga-FAPI showed an equivalent primary tumor detection to ^{18}F-FDG, but it has the additional advantage of low brain background level making it ideal for evaluating skull-base and intracranial invasion, as was shown in this study where a larger extent or a clearer border was shown on ^{68}Ga-FAPI PET than ^{18}F-FDG PET in all 8 patients with intracranial invasion, and ^{68}Ga-FAPI PET clearly visualized 4 patients with intracranial invasion. Therefore, ^{68}Ga-FAPI is superior to ^{18}F-FDG PET for exact T staging.

Radiotherapy plays an important role in NPC, so the delineation of the target area is very important [15]. The current gold standard is MRI, but it can give false-positive results because of the detection of edema and inflammation [16], and it only provides anatomic information. ^{18}F-FDG PET has limited value in locally advanced NPC patients because of physiologic uptake in a normal brain. Therefore, an alternative method is needed. In this study, when 25%SUVmax of ^{68}Ga-FAPI was utilized as a threshold for tumor volume determination, it was highly consistent with the contrast-enhanced MRI—the current gold standard. Recently, one study demonstrated that FAPI-based gross tumor volumes (GTVs) were significantly larger than conventional CT-GTVs in 14 patients with head-and-neck squamous cell carcinoma [13]. This indicates that ^{68}Ga-FAPI PET/MR may play an important role in GTV delineation in NPC patients, particularly for those with locally advanced disease. This needs to be studied in more detail in the future.

Conventional imaging techniques such as ultrasound, CT, and MR cannot accurately assess small metastatic cervical lymph nodes because their assessment based mainly on the shape and size of the lymph nodes, and the presence of necrosis [17]. ^{18}F-FDG PET/CT was reported to be more effective than conventional imaging in identifying small metastatic cervical lymph nodes [18, 19]. However, another study reported inconsistent results, for only PET/CT-positive lymph nodes, the true-positive and false-positive rates were 27% (13/48) and 73% (35/48), respectively, and no significant difference was observed for SUVmean and lymph node sizes between the true-positive and false-positive readings [20]. False positives are common for cervical lymph nodes, resulting from a high incidence of inflammation and reactive hyperplasia [20, 21]. In our study, significantly more ^{18}F-FDG-avid lymph nodes were detected than those of ^{68}Ga-FAPI (100 vs 48). Further analysis showed good correlations between ^{18}F-FDG and ^{68}Ga-FAPI uptake in paired double positive lymph nodes, which was different from that of primary tumors. Unfortunately, the imaging findings were not verified by histopathological results. These results proposed interesting questions: should the double-positive lymph nodes be considered as true metastases, and how to diagnose the only FDG-avid lymph nodes? Therefore, the difference and mechanism of ^{18}F-FDG and ^{68}Ga-FAPI uptake in primary and lymph node lesions needs to be further verified by histopathological results.

Although ^{18}F-FDG showed good diagnostic accuracy for distant malignant tumor metastases [22], ^{68}Ga-FAPI PET surprisingly detected three small skull lesions highly suspected of metastases in two patients which were missed by ^{18}F-FDG in this study. The reasons may be related to the component of activated fibroblasts and/or myofibroblasts in the osseous lesions [23]. Although none of the bone metastases could be diagnosed by histopathology, we highly suspected these lesions were metastases, because the primary NPC tumors have strong positive uptake of ^{68}Ga-FAPI, and MR signals of the skull lesions were abnormal through careful observation, and the lesions became slightly larger in the follow-up MR imaging after chemotherapy and nasopharyngeal radiotherapy (Figure 6). One pons metastasis was also detected by ^{68}Ga-FAPI rather than ^{18}F-FDG due to the low brain background of ^{68}Ga-FAPI. Interestingly, in three patients upstaged by ^{68}Ga-FAPI PET, the ^{18}F-FDG SUVmax of primary tumor is much higher than those of other patients, indicating high aggressiveness of disease. Pang reported ^{68}Ga-FAPI outperforms ^{18}F-FDG PET/CT in identifying bone metastasis in a patient with metastatic breast cancer [24]. A recent study also reported more bone metastases with higher uptake were observed on ^{68}Ga-FAPI PET/CT than ^{18}F-FDG in gastrointestinal cancers [25]. Therefore, ^{68}Ga-FAPI may be superior to ^{18}F-FDG in detecting small bone metastases.

As a new, non-specific tumor imaging agent, ^{68}Ga-FAPI showed good performance in the diagnosing and staging of NPC. However, the number of cases in this study was relatively small, and none of the lymph nodes or bone metastases were diagnosed by histopathology. Therefore, the diagnostic efficacy of ^{68}Ga-FAPI PET/MR regarding lymph nodes and bone metastases requires further investigation. The uptake mechanism of ^{68}Ga-FAPI in the primary tumor and metastases also needs further study. Despite these limitations, our preliminary study showed that ^{68}Ga-FAPI PET/MR may be a candidate for becoming a single-step staging modality for NPC.

Conclusion

In this preliminary study, ^{68}Ga-FAPI may outperform ^{18}F-FDG in the delineation of primary tumors and the detection of suspicious distant metastases because of its low background level in the brain, which suggests that simultaneous ^{68}Ga-FAPI PET/MR may serve as a single-step staging modality for patients with NPC. The N staging value of ^{68}Ga-FAPI PET is indefinite. Multi-center randomized, controlled studies using a larger patient population will be needed to further strengthen our findings in the future.

Declarations

Funding

This work was supported in part by the Key Project of National Natural Science Foundation of China (No. 81630049, 82030052), and National Key R&D Program of China (No. 2019 YFC 1316204).

Conflicts of interest:

The authors declare that they have no conflict of interest.

Ethics approval

This article does not contain any experiments with animals. All procedures involving human participants were carried out in accordance with the ethical standards of the institutional and/or national research committee and with the 1964 Helsinki Declaration and its later amendments or comparable ethical standards. This study was approved by the Clinical Research Ethics Committee of Union Hospital, Tongji Medical College, Huazhong University of Science and Technology (NO. 20200290).

Consent to participate: Informed consent was obtained from all individual participants included in

this study.

Consent for publication: Informed consent was obtained from all individual participants included in this study.

Availability of data and material: Not applicable.

Code availability: Not applicable.

References

1. Chen YP, Chan ATC, Le QT, Blanchard P, Sun Y, Ma J. Nasopharyngeal carcinoma. Lancet. 2019;394:64-80. doi:10.1016/S0140-6736(19)30956-0.
2. Lai V, Khong PL. Updates on MR imaging and ¹⁸F-FDG PET/CT imaging in nasopharyngeal carcinoma. Oral oncology. 2014;50:539-48. doi:10.1016/j.oraloncology.2013.05.005.
3. Colevas AD, Yom SS, Pfister DG, Spencer S, Adelstein D, Adkins D, et al. NCCN Guidelines Insights: Head and Neck Cancers, Version 1.2018. Journal of the National Comprehensive Cancer Network : JNCCN. 2018;16:479-90. doi:10.6004/jnccn.2018.0026.
4. Boellaard R, Delgado-Bolton R, Oyen WJ, Giammarile F, Tatsch K, Eschner W, et al. FDG PET/CT: EANM procedure guidelines for tumour imaging: version 2.0. European journal of nuclear medicine and molecular imaging. 2015;42:328-54. doi:10.1007/s00259-014-2961-x.
5. Castaldi P, Leccisotti L, Bussu F, Micciché F, Rufini V. Role of (18)F-FDG PET-CT in head and neck squamous cell carcinoma. Acta otorhinolaryngologica Italica : organo ufficiale della Societa italiana di otorinolaringologia e chirurgia cervico-facciale. 2013;33:1-8.
6. Ng SH, Chan SC, Yen TC, Chang JT, Liao CT, Ko SF, et al. Staging of untreated nasopharyngeal carcinoma with PET/CT: comparison with conventional imaging work-up. European journal of nuclear medicine and molecular imaging. 2009;36:12-22. doi:10.1007/s00259-008-0918-7.
7. Cheng Y, Bai L, Shang J, Tang Y, Ling X, Guo B, et al. Preliminary clinical results for PET/MR compared with PET/CT in patients with nasopharyngeal carcinoma. Oncology reports. 2020;43:177-87. doi:10.3892/or.2019.7392.
8. Chan SC, Yeh CH, Yen TC, Ng SH, Chang JT, Lin CY, et al. Clinical utility of simultaneous whole-body (18)F-FDG PET/MRI as a single-step imaging modality in the staging of primary nasopharyngeal carcinoma. European journal of nuclear medicine and molecular imaging. 2018;45:1297-308. doi:10.1007/s00259-018-3986-3.
9. Cao C, Yang P, Xu Y, Niu T, Hu Q, Chen X. Feasibility of multiparametric imaging with PET/MR in nasopharyngeal carcinoma: A pilot study. Oral oncology. 2019;93:91-5. doi:10.1016/j.oraloncology.2019.04.021.
10. Kratochwil C, Flechsig P, Lindner T, Abderrahim L, Altmann A, Mier W, et al. (68)Ga-FAPI PET/CT: Tracer Uptake in 28 Different Kinds of Cancer. Journal of nuclear medicine : official publication, Society of Nuclear Medicine. 2019;60:801-5. doi:10.2967/jnumed.119.227967.
11. Loktev A, Lindner T, Mier W, Debus J, Altmann A, Jäger D, et al. A Tumor-Imaging Method Targeting Cancer-Associated Fibroblasts. Journal of nuclear medicine : official publication, Society of Nuclear Medicine. 2018;59:1423-9. doi:10.2967/jnumed.118.210435.
12. Giesel FL, Kratochwil C, Lindner T, Marschalek MM, Loktev A, Lehnert W, et al. (68)Ga-FAPI PET/CT: Biodistribution and Preliminary Dosimetry Estimate of 2 DOTA-Containing FAP-Targeting Agents in Patients with Various Cancers. Journal of nuclear medicine : official publication, Society of Nuclear Medicine. 2019;60:386-92. doi:10.2967/jnumed.118.215913.
13. Syed M, Flechsig P, Liermann J, Windisch P, Staudinger F, Akbaba S, et al. Fibroblast activation protein inhibitor (FAPI) PET for diagnostics and advanced targeted radiotherapy in head and neck cancers. European journal of nuclear medicine and molecular imaging. 2020. doi:10.1007/s00259-020-04859-y.
14. Wu HB, Wang QS, Wang MF, Zhen X, Zhou WL, Li HS. Preliminary study of 11C-choline PET/CT for T staging of locally advanced nasopharyngeal carcinoma: comparison with 18F-FDG PET/CT. Journal of nuclear medicine : official publication, Society of Nuclear Medicine. 2011;52:341-6. doi:10.2967/jnumed.110.081190.

15. Co J, Mejia MB, Dizon JM. Evidence on effectiveness of intensity-modulated radiotherapy versus 2-dimensional radiotherapy in the treatment of nasopharyngeal carcinoma: Meta-analysis and a systematic review of the literature. Head & neck. 2016;38 Suppl 1:E2130-42. doi:10.1002/hed.23977.
16. Ng SH, Joseph CT, Chan SC, Ko SF, Wang HM, Liao CT, et al. Clinical usefulness of 18F-FDG PET in nasopharyngeal carcinoma patients with questionable MRI findings for recurrence. Journal of nuclear medicine : official publication, Society of Nuclear Medicine. 2004;45:1669-76.
17. Ng SH, Chang JT, Chan SC, Ko SF, Wang HM, Liao CT, et al. Nodal metastases of nasopharyngeal carcinoma: patterns of disease on MRI and FDG PET. European journal of nuclear medicine and molecular imaging. 2004;31:1073-80. doi:10.1007/s00259-004-1498-9.
18. Shen G, Xiao W, Han F, Fan W, Lin XP, Lu L, et al. Advantage of PET/CT in Target Delineation of MRI-negative Cervical Lymph Nodes In Intensity-Modulated Radiation Therapy Planning for Nasopharyngeal Carcinoma. Journal of Cancer. 2017;8:4117-23. doi:10.7150/jca.21582.
19. Peng H, Chen L, Tang LL, Li WF, Mao YP, Guo R, et al. Significant value of (18)F-FDG-PET/CT in diagnosing small cervical lymph node metastases in patients with nasopharyngeal carcinoma treated with intensity-modulated radiotherapy. Chinese journal of cancer. 2017;36:95. doi:10.1186/s40880-017-0265-9.
20. Lee SH, Huh SH, Jin SM, Rho YS, Yoon DY, Park CH. Diagnostic value of only 18F-fluorodeocyglucose positron emission tomography/computed tomography-positive lymph nodes in head and neck squamous cell carcinoma. Otolaryngology–head and neck surgery : official journal of American Academy of Otolaryngology-Head and Neck Surgery. 2012;147:692-8. doi:10.1177/0194599812443040.
21. Tsai MC, Shu YC, Hsu CC, Lin CK, Lee JC, Chu YH, et al. False-positive finding of retropharyngeal lymph node recurrence in both fluorine (18)FDG PET and MRI in a patient with nasopharyngeal carcinoma. Head & neck. 2016;38:E84-6. doi:10.1002/hed.24205.
22. Shen G, Zhang W, Jia Z, Li J, Wang Q, Deng H. Meta-analysis of diagnostic value of 18F-FDG PET or PET/CT for detecting lymph node and distant metastases in patients with nasopharyngeal carcinoma. The British journal of radiology. 2014;87:20140296. doi:10.1259/bjr.20140296.
23. Dohi O, Ohtani H, Hatori M, Sato E, Hosaka M, Nagura H, et al. Histogenesis-specific expression of fibroblast activation protein and dipeptidylpeptidase-IV in human bone and soft tissue tumours. Histopathology. 2009;55:432-40. doi:10.1111/j.1365-2559.2009.03399.x.
24. Pang Y, Zhao L, Chen H. 68Ga-FAPI Outperforms 18F-FDG PET/CT in Identifying Bone Metastasis and Peritoneal Carcinomatosis in a Patient With Metastatic Breast Cancer. Clinical nuclear medicine. 2020;45:913-5. doi:10.1097/rlu.0000000000003263.
25. Pang Y, Zhao L, Luo Z, Hao B, Wu H, Lin Q, et al. Comparison of (68)Ga-FAPI and (18)F-FDG Uptake in Gastric, Duodenal, and Colorectal Cancers. Radiology. 2020:203275. doi:10.1148/radiol.2020203275.

Tables

Table 1. Clinical information and TNM staging for all patients

No.	Sex	Age	Diagnosis	WHO classification	T Stage			N stage			M stage			Overall Stage			FAPI Staging change#
					MR	FDG	FAPI	MR	FDG	FAPI	MR	FDG	FAPI	MR	FDG	FAPI	
1	M	41	ND	I	T1	T1	T1	N1	N2	N1	M1	M0	M1	IVB	III	IVB	Up
2	F	56	ND	NA*	T3	T3	T3	N1	N2	N1	M1	M0	M1	IVB	III	IVB	Up
3	M	63	ND	III	T4	T3	T4	N1	N2	N1	M1	M0	M1	IVB	III	IVB	Up
4	M	69	ND	I	T1	T1	T1	N1	N2	N2	M0	M0	M0	II	III	III	None
5	F	40	ND	III	T1	T1	T1	N0	N1	N1	M0	M0	M0	I	II	II	None
6	M	48	ND	II	T2	T2	T2	N3	N3	N3	M0	M0	M0	IVA	IVA	IVA	None
7	M	46	ND	III	T2	T2	T2	N3	N3	N3	M0	M0	M0	IVA	IVA	IVA	None
8	M	58	ND	III	T3	T3	T3	N2	N2	N2	M0	M0	M0	III	III	III	None
9	F	58	ND	III	T3	T3	T3	N1	N2	N1	M0	M0	M0	III	III	III	None
10	F	49	ND	III	T4	T4	T4	N1	N3	N1	M0	M0	M0	IVA	IVA	IVA	None
11	M	62	ND	I	T4	T4	T4	N1	N2	N2	M0	M0	M0	IVA	IVA	IVA	None
12	F	53	Recurrence	NA**	T4	T4	T4	N0	N0	N0	M0	M0	M0	IVA	IVA	IVA	None
13	F	50	ND	III	T2	T2	T2	N1	N3	N1	M0	M0	M0	II	IVA	II	Down
14	M	36	ND	II	T2	T2	T2	N1	N2	N1	M0	M0	M0	II	III	II	Down
15	F	39	ND	III	T3	T3	T3	N2	N3	N2	M0	M0	M0	III	IVA	III	Down

ND = New diagnosed; FDG = ^{18}F-FDG; FAPI = ^{68}Ga-FAPI

*Non-keratinizing carcinoma, unknown differentiated condition; **recurrent NPC with unknown pathological type

#Compared with ^{18}F-FDG

Table 2 Visual evaluation of primary tumor invasion with two tracers (No. of patients equivalent to MR).

Lesion Invasion	MR detection	FDG=MR	FAPI=MR	FAPI=FDG	FAPI>FDG	FAPI<FDG
Nasopharynx	15	15	15	5	6	4
Parapharyngeal space	12	10	12	2	5	5
Skull Base	8	0	7	0	8	0
Intracranial Invasion	4	0	4	0	4	0

Table 3. Comparison of the primary tumor and lymph node uptake between ^{18}F-FDG and ^{68}Ga-FAPI PET/MR.

	Primary tumor		Positive lymph node	
	^{18}F-FDG positive	^{68}Ga-FAPI positive	^{18}F-FDG positive	^{68}Ga-FAPI positive
No. of patients	15	15	14	14
No. of lesions	15	15	100	48
Paired lesions	15		48	
SUVmax	17.73±6.84	13.87±5.13	11.94±6.15	8.81±3.79
p	0.078		0.000	

Table 4. Comparison of primary tumor volume measured by enhanced MR, T2-weighted images, FDG, and FAPI PET with a different threshold.

Modalities and Thresholds		Tumor volume (cm^3)
MR	MR+C	17.09±10.61
	T2WI	17.54±9.02
^{68}Ga-FAPI	20% SUVmax	21.95±11.62
	25% SUVmax	17.95±10.52
	30% SUVmax	15.07±9.34
^{18}F-FDG	20% SUVmax	18.22±11.46
	25% SUVmax	14.81±9.8
	30% SUVmax	12.45±8.51

Table 5. Intra-group correlation analysis of the primary tumor volume measured by contrast-enhanced MR, T2-weighted images, and FDG/FAPI with different thresholds.

		T2WI	FAPI20%	FAPI25%	FAPI30%	FDG20%	FDG25%	FDG30%
MR+C	ICC	0.93	0.82	0.88	0.84	0.91	0.89	0.80
	95% CI	0.79-0.98	0.27-0.95	0.67-0.96	0.59-0.95	0.75-0.97	0.67-0.96	0.16-0.95
T2WI	ICC	-	0.78	0.86	0.83	0.85	0.83	0.73
	95% CI	-	0.30-0.93	0.64-0.95	0.56-0.94	0.60-0.95	0.51-0.94	0.10-0.92

ICC: interclass correlation coefficient; CI: confidence interval

Figures

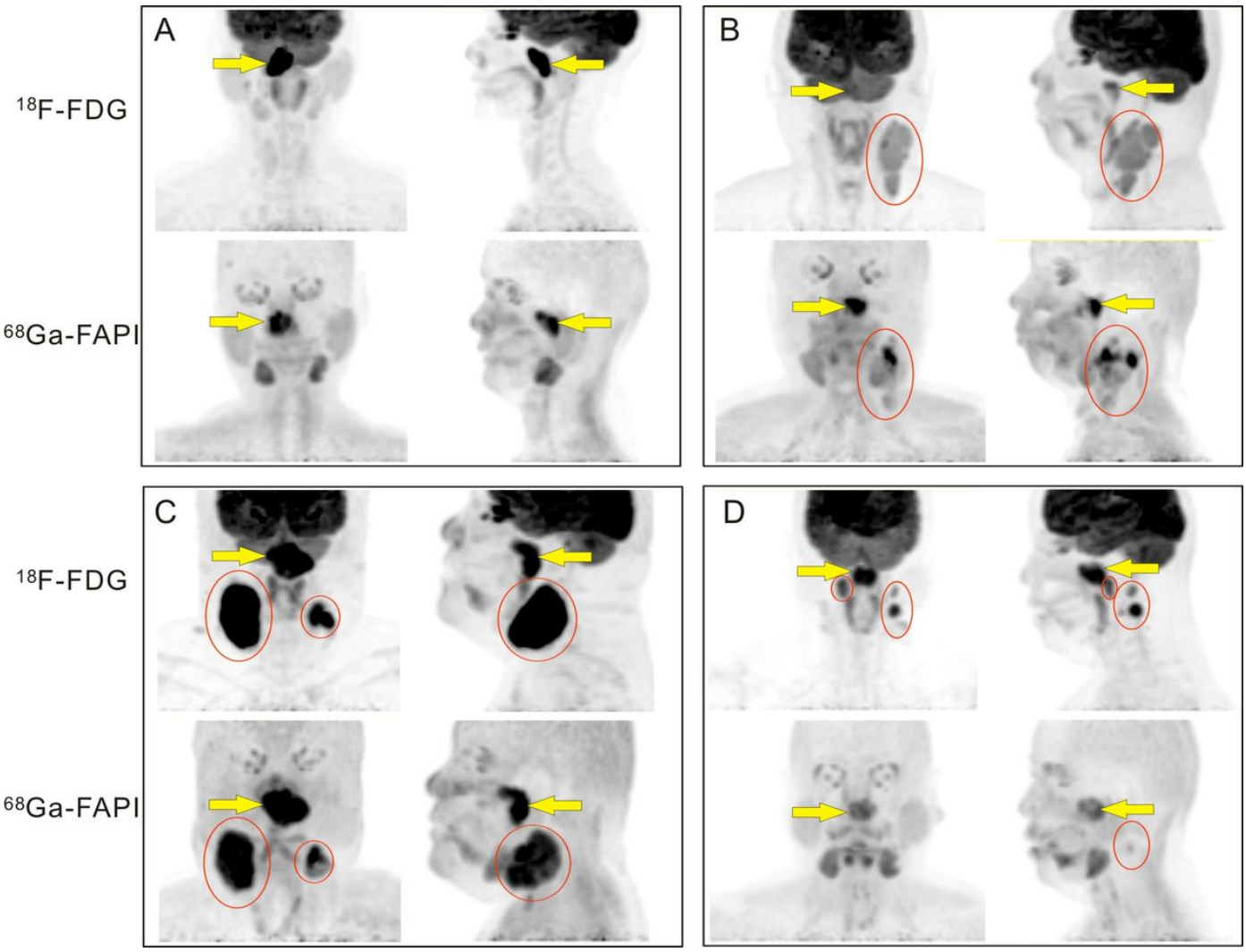

Figure 1

Comparison of anterior and lateral head-neck maximum-intensity projections (MIP) in four representative patients (Patients 2, 6, 7, and 13 from A to D, respectively). Physiologic uptake is seen in the brain, ocular muscles, salivary glands, and pharyngeal glands on 18F-FDG MIP (1st and 3rd rows), but only in ocular muscles and salivary glands on 68Ga-FAPI MIP with low brain background levels (2nd and 4th rows). (A) 18F-FDG reveals the primary tumor (arrows) more clearly than 68Ga-FAPI. (B) 68Ga-FAPI reveals the primary tumor (arrows) more clearly than 18F-FDG, and provides more details regarding the heterogeneity of nodal metastases (circles). (C) Both images show a similar effect between the primary foci (arrows) and the lymph nodes (circles). (D) 18F-FDG delineates clearer primary tumor (arrows) and more metastatic lymph nodes (circles) than 68Ga-FAPI.

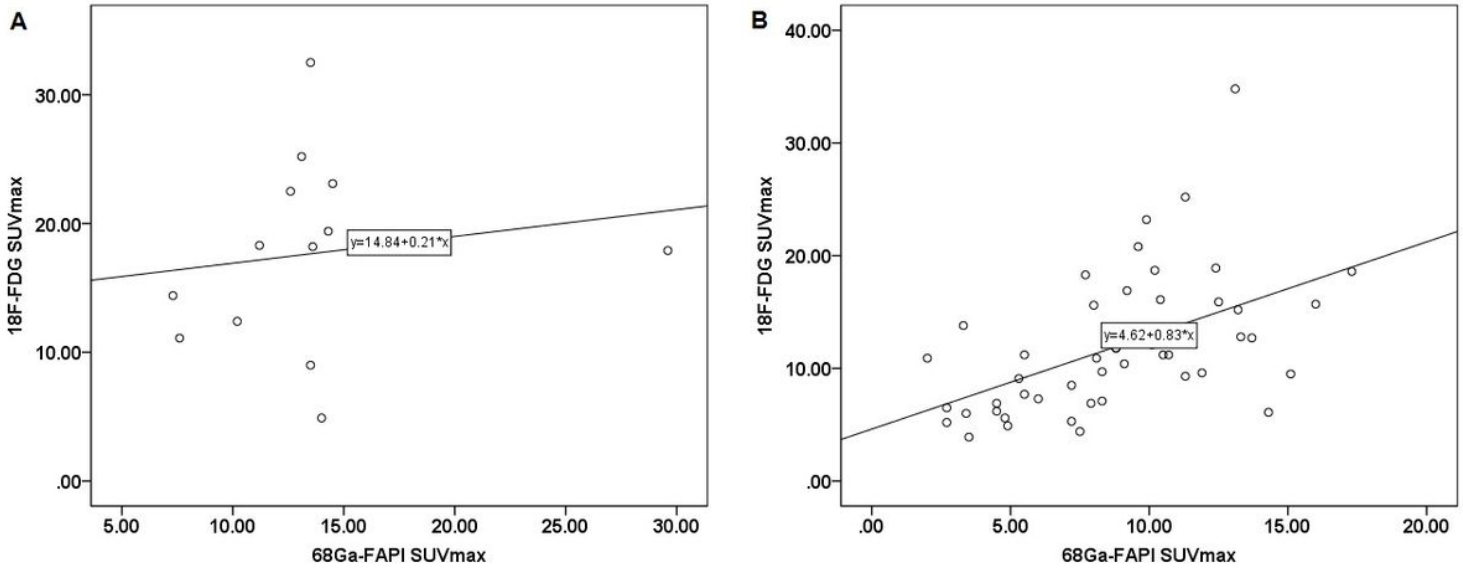

Figure 2

Comparison of SUVmax of 68Ga-FAPI and 18F-FDG in the primary tumor (A, r = 0.227, p=0.416) and matched double positive lymph nodes (B, r =0.5122, p = 0.000).

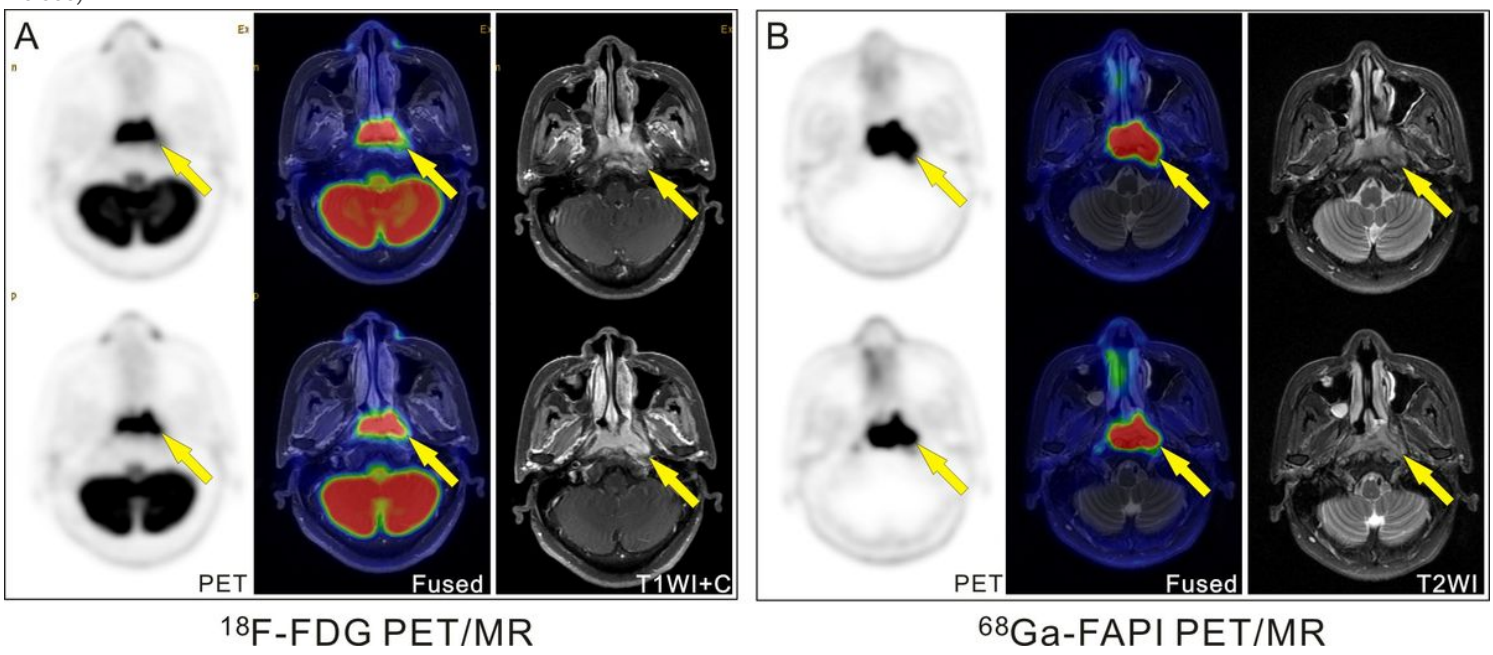

Figure 3

A 58-year-old woman with nonkeratinizing undifferentiated carcinoma of the nasopharynx (Patient 9). 18F-FDG PET/MR (A) and 68Ga-FAPI PET/MR (B) both demonstrate intense tracer uptake at the NPC primary site and parapharyngeal space invasion (arrows). However, the extent of the parapharyngeal space invasion is larger with 68Ga-DOTA-FAPI PET than with 18F-FDG PET, in line with the MR images.

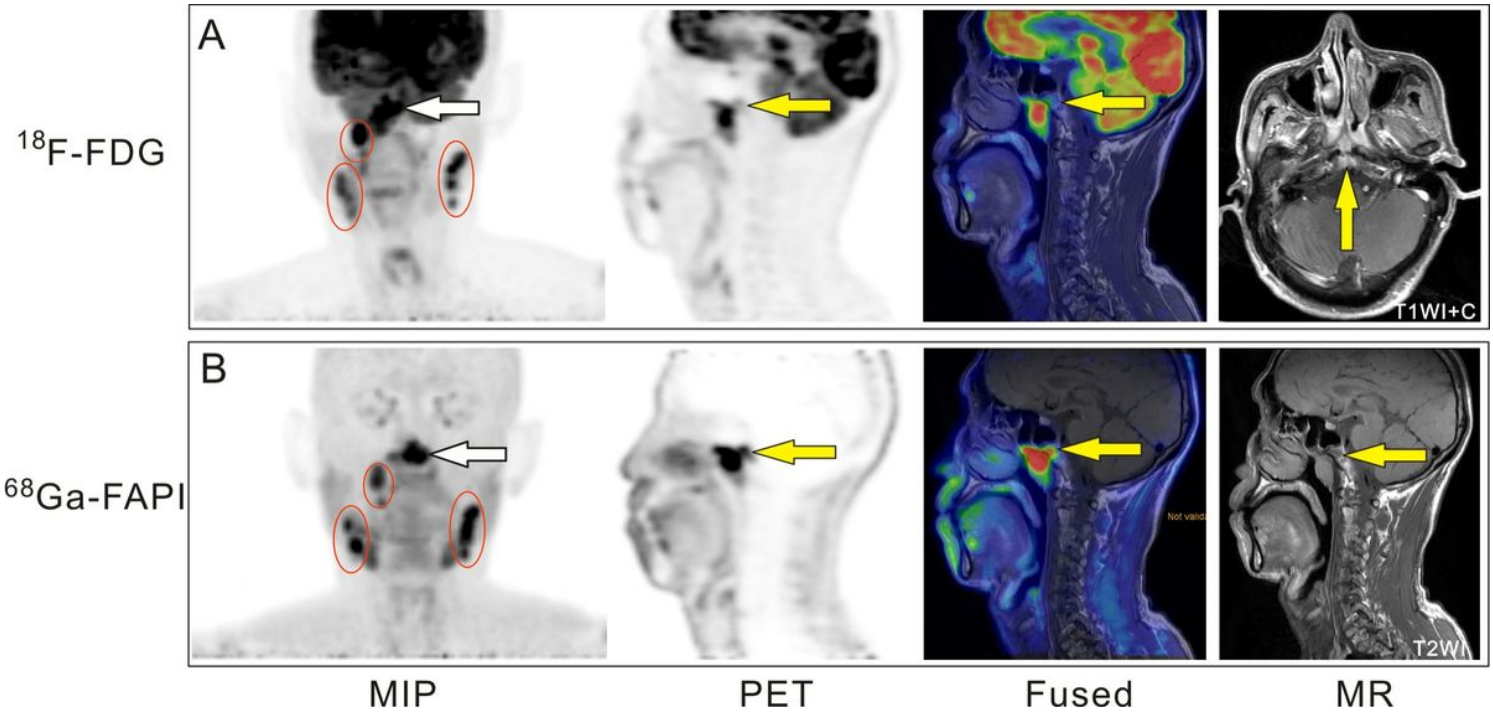

Figure 4

A 58-year-old man with nonkeratinizing undifferentiated carcinoma of the nasopharynx (Patient 8). 68Ga-FAPI PET/MR (A) and 18F-FDG PET/MR (B) both demonstrate intense tracer uptake at the NPC primary site (white arrow) and at multiple lymph nodes (circles) on both sides of the neck. 68Ga-FAPI PET/MR revealed the involvement of the occipital slope (yellow arrow) more clearly than 18F-FDG.

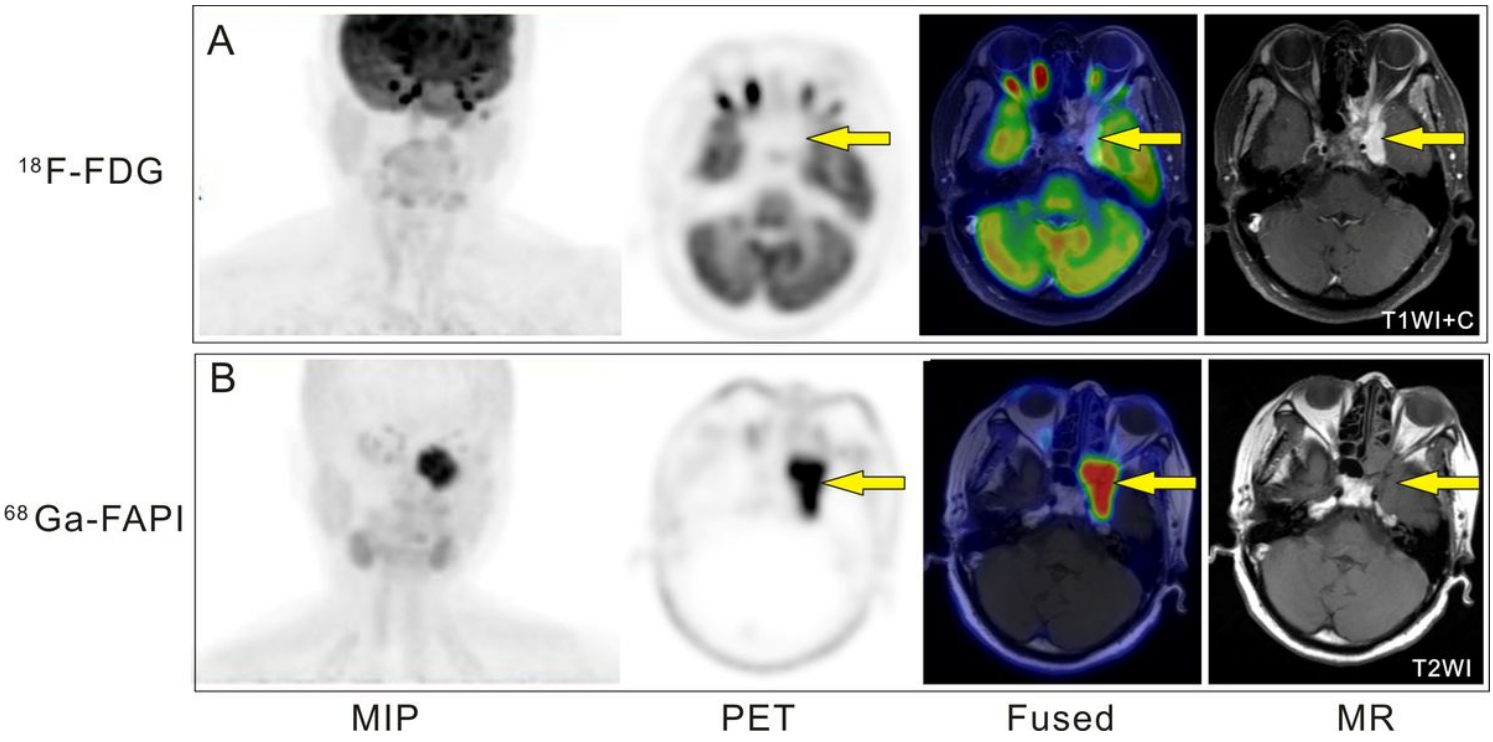

Figure 5

A 53-year-old woman with recurrent NPC of the left nasopharynx (Patient 12). The uptake of 18F-FDG in the skull base and left temporal lobe is not shown clearly (A). 68Ga-FAPI PET/MR (B) shows intense uptake of 68Ga-FAPI in the skull base and the adjacent left temporal lobe (arrow, SUVmax 14.0), with clear borders, matched with enhanced MR.

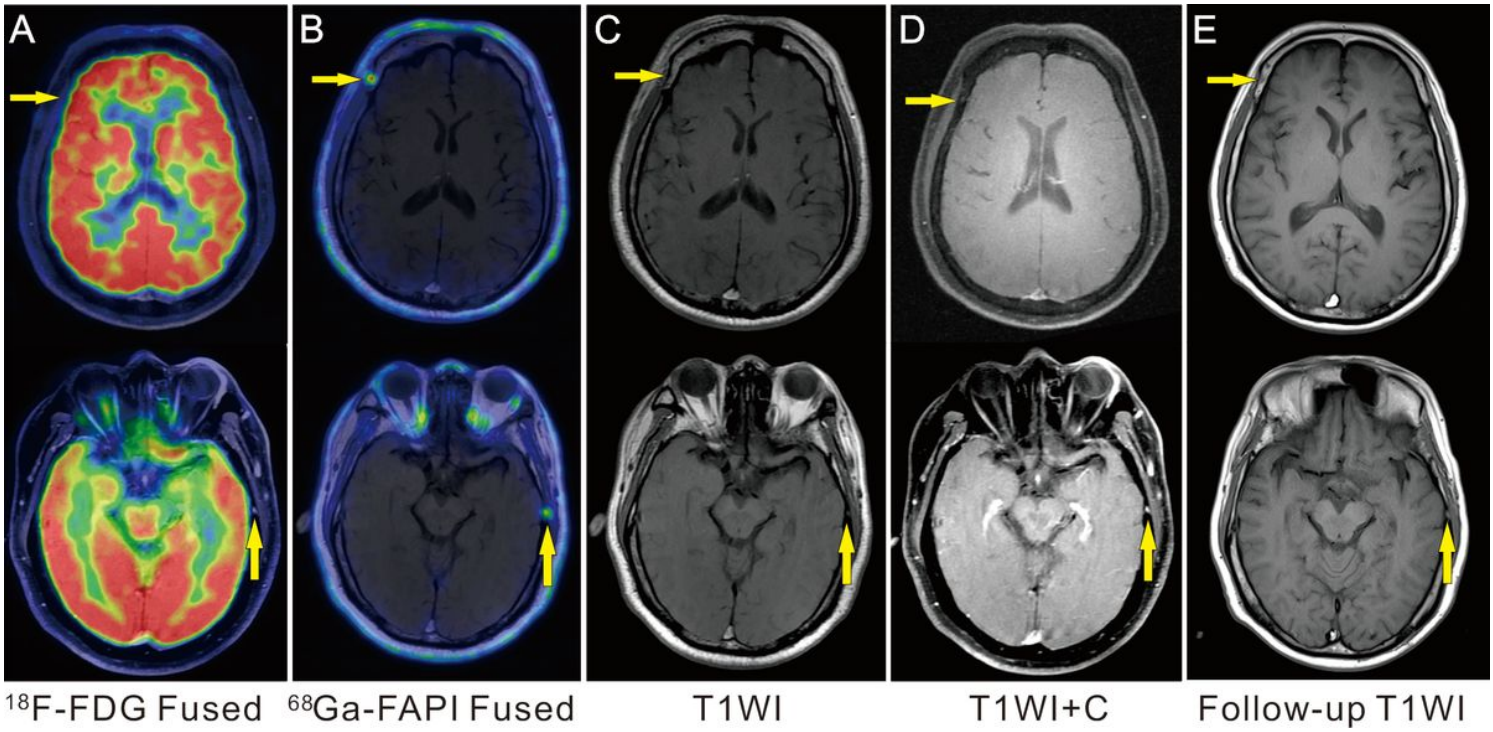

Figure 6

A 41-year-old man with keratinizing squamous cell carcinoma of the nasopharynx (Patient 1). (A) 18F-FDG didn't show any increased uptake in the skull. (B) 68Ga-FAPI revealed two small skull lesions, which were initially missed by MR and can be identified on both T1-weighted and contrast enhanced images after careful observation (C–D). The skull lesions became slightly larger on the follow-up T1-weighted MR images after chemotherapy and radiotherapy 4 months later (E). These skull lesions were highly suspected of metastases.